Global analysis of the pMSSM in light of the Fermi GeV excess: prospects for the LHC Run-II and astroparticle experiments

JCAP04(2016)037

(http://iopscience.iop.org/1475-7516/2016/04/037)

Journal of Cosmology and Astroparticle Physics
An IOP and SISSA journal

Global analysis of the pMSSM in light of the Fermi GeV excess: prospects for the LHC Run-II and astroparticle experiments

Gianfranco Bertone,[a] **Francesca Calore,**[a] **Sascha Caron,**[b,c] **Roberto Ruiz,**[d] **Jong Soo Kim,**[e] **Roberto Trotta**[f,g] **and Christoph Weniger**[a]

[a]GRAPPA, University of Amsterdam,
Science Park 904, 1090 GL Amsterdam, Netherlands
[b]IMAPP, Radboud University Nijmegen,
P.O. Box 9010, NL-6500 GL Nijmegen, The Netherlands
[c]Nikhef,
Science Park 105, 1098XG Amsterdam, The Netherlands
[d]Instituto de Física Corpuscular, IFIC-UV/CSIC, University of Valencia,
Apartado 22085, E-46071 València, Spain
[e]Instituto de Física Teórica UAM/CSIC, Universidad Autónoma de Madrid,
Cantoblanco, E-28049, Madrid, Spain
[f]Imperial Centre for Inference and Cosmology,
Imperial College London, Blackett Laboratory,
Prince Consort Road, London SW7 2AZ, U.K.
[g]Data Science Institute, William Penney Laboratory, Imperial College London,
London SW7 2AZ, U.K.

E-mail: gf.bertone@gmail.com, f.calore@uva.nl, scaron@nikhef.nl, roberto.ruiz@ific.uv.es, jongsoo.kim@tu-dortmund.de, r.trotta@imperial.ac.uk, c.weniger@uva.nl

Received November 14, 2015
Revised March 16, 2016
Accepted March 23, 2016
Published April 18, 2016

doi:10.1088/1475-7516/2016/04/037

JCAP04(2016)037

Abstract. We present a new global fit of the 19-dimensional phenomenological Minimal Supersymmetric Standard Model (pMSSM-19) that complies with all the latest experimental results from dark matter indirect, direct and accelerator dark matter searches. We show that the model provides a satisfactory explanation of the excess of gamma rays from the Galactic centre observed by the *Fermi* Large Area Telescope, assuming that it is produced by the annihilation of neutralinos in the Milky Way halo. We identify two regions that pass all the constraints: the first corresponds to neutralinos with a mass $\sim 80 - 100\,\mathrm{GeV}$ annihilating into WW with a branching ratio of 95%; the second to heavier neutralinos, with mass $\sim 180 - 200\,\mathrm{GeV}$ annihilating into $\bar{t}t$ with a branching ratio of 87%. We show that neutralinos compatible with the Galactic centre GeV excess will soon be within the reach of LHC run-II — notably through searches for charginos and neutralinos, squarks and light smuons — and of Xenon1T, thanks to its unprecedented sensitivity to spin-dependent cross-section off neutrons.

Keywords: dark matter detectors, dark matter theory, gamma ray experiments, supersymmetry and cosmology

ArXiv ePrint: 1507.07008

JCAP04(2016)037

Contents

1 Introduction

The existence of dark matter (DM) is now robustly established [1–4] and its cosmological abundance measured with high precision [5]. Yet, the fundamental nature of the most abundant matter component in the Universe is unknown. According to the most promising theories, DM is a *new fundamental particle*. As a consequence, the search for DM is also a search for new physics beyond that of the well-known elementary particles, as laid down in the Standard Model (SM). Weakly interacting massive particles (WIMPs) are the leading DM candidates: they arise in many extensions of the Standard Model of particle physics, and naturally achieve the appropriate relic density through self-annihilation in the early Universe. WIMPs can be searched for with three detection strategies: direct detection of the energy recoil of nuclei scattering off DM particles; indirect detection of the final stable products of DM annihilation or decay, as for example gamma rays; and accelerator searches for new particles, in particular at the Large Hadron Collider (LHC).

An excess in the gamma-ray emission from the centre of our Galaxy has been discovered in data from the Large Area telescope (LAT), aboard the *Fermi* satellite [6–16]. The nature of the so-called *Fermi* GeV excess remains a mystery. Several explanations have been put forward, the most exciting of which is perhaps DM annihilation in the halo of the Milky Way (see for example [13, 14, 17]). Astrophysical processes have also been suggested: the emission from a population of dim unresolved sources [18–21], and the inverse Compton emission from a new population of cosmic rays, either from time-dependent events taking place in the past of the Galaxy [22–24] or from the high star formation activity in the inner Galaxy [25].

Very recently, two reanalyses of the gamma-ray emission from the inner Galaxy found strong evidence for the *Fermi* GeV excess being due to hundreds to thousands of dim unresolved point sources [26, 27], most likely millisecond pulsars [18]. Even more recently, it was shown that part or all of the required millisecond pulsar population could originate from the disruption of globular clusters by tidal forces in the inner Galaxy [28]. Directly detecting some of the millisecond pulsars in the inner Galaxy by radio observations is the next critical step for fully establishing this scenario [26].

JCAP04(2016)037

It is however striking that the *Fermi* GeV excess spectrum and spatial distribution are well fitted by what is expected from DM annihilation. The excess could be the first non-gravitational signal of DM particles. It is thus urgent to either corroborate or disprove the DM particle nature of the *Fermi* GeV excess in the framework of concrete models for physics beyond the SM. Supersymmetry (SUSY) is one of the best-motivated classes of renormalizable extensions of the SM, which can accommodate a stable DM particle together with new degrees of freedom that mediate interactions. The most generic R-parity conserving and phenomenologically viable supersymmetric model is the phenomenological Minimal Supersymmetric Standard Model (pMSSM) [29]. In this work we address the following key question: can models of the pMSSM explain the observed properties of the *Fermi* GeV excess, while retaining consistency with other experimental data? And if so, what are the detection prospects for future direct detection and collider experiments?

Until now, MSSM scenarios [30] could not reproduce the *Fermi* GeV excess as observed by [14], as it was impossible to obtain in this framework a light neutralino ($m_\chi \sim 30$–$40\,\mathrm{GeV}$), as required to fit the *Fermi* GeV excess spectrum, which could also account for the cosmological DM as measured by Planck [5]. However, [15] demonstrated that higher WIMP masses and annihilation channels different from b-quark pairs can give a good fit to the *Fermi* excess, owing to the freedom allowed by background model systematics. By fitting the GeV excess data of [15], it has been shown that viable solutions in the MSSM exist [31]. In the context of the pMSSM, [32] demonstrated that a re-assessment of the theoretical uncertainties in the DM signal spectra opens up a new phenomenology at the LHC experiments. Here we present the *first* systematic study of the pMSSM parameter space through global fitting techniques. This approach exhaustively covers all possible phenomenological signatures, allowing us a complete overview of the viable pMSSM interpretation of the *Fermi* GeV excess.

The paper is organized as follows: in section 2 we briefly present the well-known framework of the pMSSM and the parameters describing the model. In section 3 we describe the experimental set-up of the global fit and the implementation of the joint likelihood. We present the results of the parameter scan in section 4. We then discuss the implications for future direct and indirect detection experiments in section 5.1 and the prospects for detection at the LHC run II in section 5.2. Finally, we summarize our conclusions in section 6.

2 The theoretical framework: the pMSSM

We here study the pMSSM [29], in which the number of free parameters can be reduced to 19, given the present lack of experimental evidence for SUSY and no experimental indication that one requires the full freedom of a 22-dimensional pMSSM at present.

In this model, the lightest supersymmetric particle (LSP) is the lightest neutralino, χ, a combination of the neutral electroweak gauginos and higgsinos fields. The neutralino is one of the most well-motivated particle DM candidates since it is neutral, stable over cosmological timescales and can lead naturally to the correct DM relic abundance in the early Universe. In what follow, we assume that the neutralino is the particle DM candidate although we do not impose it to fully account for the DM relic abundance as measured by Planck but we allow for subdominant contributions to the DM content (cf. section 3).

We assume first and second generation mass universality, separately in the lepton and quark sectors (table 1). The trilinear couplings of the sfermions enter in the off-diagonal parts of the sfermion mass matrices. Since these entries are proportional to the Yukawa couplings of the respective fermions, we approximate the trilinear couplings associated with the first and second generation fermions to be zero, while the parameters A_t, A_b and A_τ represent the third

JCAP04(2016)037

pMSSM parameters and priors			
Flat priors		Log priors	
M_1 [TeV]	(-5, 5)	$\mathrm{sgn}(M_1)\log\lvert M_1\rvert/\mathrm{GeV}$	$(-3.7, 3.7)$
M_2 [TeV]	(0.1, 5)	$\log M_2/\mathrm{GeV}$	$(2, 3.7)$
M_3 [TeV]	(-5, 5)	$\mathrm{sgn}(M_3)\log\lvert M_3\rvert/\mathrm{GeV}$	$(-3.7, 3.7)$
m_L [TeV]	(0.1,4)	$\log m_L/\mathrm{GeV}$	$(-1, 3.6)$
m_E [TeV]	(0.1,4)	$\log m_E/\mathrm{GeV}$	$(-1, 3.6)$
m_{L_3} [TeV]	(0.1,4)	$\log m_{L_3}/\mathrm{GeV}$	$(-1, 3.6)$
m_{E_3} [TeV]	(0.1,4)	$\log m_{E_3}/\mathrm{GeV}$	$(-1, 3.6)$
m_Q [TeV]	(0.1,4)	$\log m_Q/\mathrm{GeV}$	$(-1, 3.6)$
m_U [TeV]	(0.1,4)	$\log m_U/\mathrm{GeV}$	$(-1, 3.6)$
m_D [TeV]	(0.1,4)	$\log m_D/\mathrm{GeV}$	$(-1, 3.6)$
m_{Q_3} [TeV]	(0.1,4)	$\log m_{Q_3}/\mathrm{GeV}$	$(-1, 3.6)$
m_{U_3} [TeV]	(0.1,4)	$\log m_{U_3}/\mathrm{GeV}$	$(-1, 3.6)$
m_{D_3} [TeV]	(0.1,4)	$\log m_{D_3}/\mathrm{GeV}$	$(-1, 3.6)$
A_t [TeV]	(-10, 10)	$\mathrm{sgn}(A_t)\log\lvert A_t\rvert/\mathrm{GeV}$	$(-4, 4)$
A_b [TeV]	(-10,10)	$\mathrm{sgn}(A_0)\log\lvert A_b\rvert/\mathrm{GeV}$	$(-4, 4)$
A_τ [TeV]	(-10,10)	$\mathrm{sgn}(A_0)\log\lvert A_\tau\rvert/\mathrm{GeV}$	$(-4, 4)$
μ [TeV]	(-5,5)	$\mathrm{sgn}(\mu)\log\lvert\mu\rvert/\mathrm{GeV}$	$(-3.7, 3.7)$
m_A [TeV]	(0.01, 5)	$\log m_A/\mathrm{GeV}$	$(1, 3.7)$
$\tan\beta$	$(2, 62)$	$\tan\beta$	$(2, 62)$
M_t [GeV]	173.2 ± 0.87 [33] (Gaussian prior)		
ρ_0 [GeV/cm^3]	0.4 ± 0.1 [34] (Gaussian prior)		

Table 1. pMSSM parameters and top mass value used in this paper and the prior range for the two prior choices adopted in our scans. "Flat priors" are uniform on the parameter itself (within the ranges indicated), while "Log priors" are uniform in the log of the parameter (within the ranges indicated).

generation trilinear couplings. In our set-up, the Higgs sector is fully described by the ratio of the Higgs vacuum expectation values $\tan\beta$, the higgsino mass parameter μ and the mass of the pseudoscalar Higgs m_A, which are more directly related to the phenomenology of the model. This 19-dimensional realization of the pMSSM encapsulates all phenomenologically relevant features of the full model that are of interest for DM and collider experiments. The model parameters are displayed in table 1, along with their prior ranges. All of the input parameters are defined at the SUSY scale $\sqrt{m_{\tilde{t}_1} m_{\tilde{t}_2}}$.

3 The experimental setup

We implement experimental constraints with a joint likelihood function, whose logarithm takes the following form:

$$\begin{aligned}\ln\mathcal{L}_{\mathrm{Joint}} = \ln\mathcal{L}_{\mathrm{GCE}} + \ln\mathcal{L}_{\mathrm{EW}} + \ln\mathcal{L}_{\mathrm{B(D)}} + \ln\mathcal{L}_{\Omega_\chi h^2} \\ + \ln\mathcal{L}_{\mathrm{LUX}} + \ln\mathcal{L}_{\mathrm{IC}} + \ln\mathcal{L}_{\mathrm{Higgs}} + \ln\mathcal{L}_{\mathrm{SUSY}},\end{aligned} \tag{3.1}$$

JCAP04(2016)037

where $\mathcal{L}_{\rm GCE}$ represents the *Fermi* GeV excess, $\mathcal{L}_{\rm EW}$ electroweak precision observables, $\mathcal{L}_{\rm B(D)}$ B and D physics constraints, $\mathcal{L}_{\Omega_\chi h^2}$ measurements of the cosmological DM relic density, $\mathcal{L}_{\rm LUX}$ ($\mathcal{L}_{\rm IC}$) direct (indirect) DM detection constraints and $\mathcal{L}_{\rm Higgs}$ ($\mathcal{L}_{\rm SUSY}$) Higgs (sparticles) searches at colliders. We discuss each component in turn:

$\mathcal{L}_{\rm GCE}$: for the *Fermi* GeV excess likelihood we follow the treatment in [15], to account astrophysical uncertainties. In addition, we include uncorrelated 10% uncertainties as DM modeling systematics, following ref. [32]. We marginalize the likelihood function over the uncertainties in the Galactic centre J-value, which is assumed to follow a log-normal distribution with mean $\log_{10} J/(\mathrm{GeV}^2\,\mathrm{cm}^{-5}\,\mathrm{sr}^{-1}) = 23.29$ and variance $\Delta \log_{10} J/(\mathrm{GeV}^2\,\mathrm{cm}^{-5}\,\mathrm{sr}^{-1}) = 0.37$ [17]. When the predicted neutralino relic density, Ω_χ, is smaller than the Planck measurement, $\Omega_{\rm DM}$, we follow [35] and adopt the so-called "scaling Ansatz", i.e. we assume that the local ratio of neutralino (ρ_χ) to total DM densities ($\rho_{\rm DM}$) is equal to that for their cosmic abundances:

$$\rho_\chi/\rho_{\rm DM} = \Omega_\chi/\Omega_{\rm DM} \equiv f_\chi. \tag{3.2}$$

$\mathcal{L}_{\rm EW}$: this implements constraints from Z-pole measurements at LEP [36]. We include the constraint on the effective electroweak mixing angle for leptons $\sin^2\theta_{\rm eff}$, the total width of the Z-boson Γ_Z, the hadronic pole cross-section σ^0_{had}, as well as the decay width ratios R^0_l, R^0_c and the asymmetry parameters A_l, A_b, A_c and $A^{0,l}_{FB}$, $A^{0,c}_{FB}$. In addition, we also use the measurement of the mass of the W boson m_W from the LEP experiment [36]. We apply a Gaussian likelihood for all of these quantities, with mean and standard deviation as given in table II of [37].

$\mathcal{L}_{\rm B(D)}$: the flavor observables related with B and D physics considered are $BR(\bar{B} \to X_s\gamma)$, $R_{\Delta M_{B_s}}$, $\frac{BR(B_u\to\tau\nu)}{BR(B_u\to\tau\nu)_{SM}}$, Δ_{0-}, $BR(D_s \to \tau\nu)$, R_{l23}, $BR(\overline{B}_s \to \mu^+\mu^-)$ and $BR(\overline{B}_d \to \mu^+\mu^-)$. For all we apply a Gaussian likelihood and for most of them we use the measurements following table II of [37]. The experimental values assumed for $BR(\overline{B}_s \to \mu^+\mu^-)$ and $BR(\overline{B}_d \to \mu^+\mu^-)$ are $(2.9 \pm 0.8) \times 10^{-9}$ and $(3.6 \pm 1.55) \times 10^{-10}$ (theoretical uncertainties included [38]) [39] respectively.

$\mathcal{L}_{\Omega_\chi h^2}$: we include the Planck Cosmic Microwave Background data constraint on the DM relic abundance as an upper limit, to allow for the possibility that neutralinos are a subdominant DM component. We follow the formalism in the appendix of [40], using as central value the result from Planck temperature and lensing data $\Omega_\chi h^2 = 0.1186 \pm 0.0031$ [41] with a (fixed) theoretical uncertainty, $\tau = 0.012$, to account for the numerical uncertainties entering in the calculation of the relic density.

$\mathcal{L}_{\rm LUX}$: for DM direct detection we include upper limits from the LUX experiment [42], as implemented in the LUXCalc code [43], including both the spin-independent (SI) and spin-dependent (SD) cross-sections in the event rate calculation. We adopt hadronic matrix elements determined by lattice QCD [44, 45].

$\mathcal{L}_{\rm IC}$: this implements conservative upper limits on the proton spin-dependent cross-section from the IceCube detector in its 79-string configuration [46] (IC-79). Comparable — if slightly weaker — limits have been set for the WW channel by Super-Kamiokande [47] and ANTARES [48]. The most stringent constraint is for the case where WIMPs annihilate exclusively to WW pairs. Since the neutrino spectrum generated by Z bosons is similar to the W bosons we apply this constraint whenever the combined branching fraction to WW

JCAP04(2016)037

and ZZ is above 95%. In that case the likelihood is a step function smeared with half a Gaussian (as in eq. (3.5) of [49]) to account for theoretical and experimental uncertainties that we set to be 50% of the predicted value.

$\mathcal{L}_{\text{Higgs}}$: the likelihood for the Higgs searches has two components: the first implements bounds obtained from Higgs searches at LEP, Tevatron and LHC via HiggsBounds [50], which returns whether a model is excluded or not at the 95% CL. The second component constrains the mass and the production times decay rates of the Higgs-like boson discovered by the LHC experiments ATLAS [51] and CMS [52]. We use HiggsSignals [53] assuming a theoretical uncertainty in the lightest Higgs mass calculation of 2 GeV.

$\mathcal{L}_{\text{SUSY}}$: SUSY searches constraints at LEP and Tevatron follow the likelihood used in [49]. We have imposed the strict constraints from a large number of searches for SUSY at the LHC experiments. The branching ratios of the sparticles have been calculated with SUSYHIT 1.5 [54]. We have generated the hadronized event samples with Pythia 8.2 [55] and have employed the NNPDF 2.3 parton distribution functions [56]. The generated events are passed on to CheckMATE [57], which is based on the fast detector simulation Delphes 3.10 [58]. CheckMATE tests if the model point in question is excluded or not at 95% confidence level by comparing to current experimental searches at the LHC for supersymmetry in the relevant hadronic and leptonic final states with large missing transverse momentum. We assign a 0 log-likelihood $\mathcal{L}_{\text{SUSY}} = 0$ if the point passes all constraints, and exclude it if it fails any of them.

We have only included observables we consider robust in order to be conservative. For instance, we have dropped the electroweak precision observables R_b^0 and $A_{FB}^{0,b}$ in the fit because it is unclear whether the large deviations of 2.5σ that are observed with respect to the SM predictions are due to unknown systematic uncertainties or to new physics. The experimental status of the magnetic anomaly of the muon, $a_\mu = \frac{1}{2}(g-2)_\mu$ remains unclear in the face of persistent discrepancies in the determination of the hadronic vacuum-polarization diagram using either e^+e^- or the hadronic $\tau-$decay data. We do not include DM searches in dwarf spheroidal galaxies by the *Fermi*-LAT [59], as constraints are given only for 100% branching ratio into specific final states.

Finally, we refer to [37] for details about how the SUSY spectrum and observables are computed.

We use the MultiNest [60] algorithm as implemented in SuperBayeS-v2.0, to perform a global fit of the pMSSM parameter space, including all the data in eq. (3.1), excepting the SUSY searches at the LHC. This is because the LHC searches evaluation is computationally too expensive to be performed on-the-fly. Our scans were run using both log and flat priors to ensure a complete coverage of the parameter space, gathering $\sim 10^6$ samples from $\sim 10^8$ likelihood evaluations. Samples have been thinned by a factor of 10, focusing our search to regions of the parameter space that were not clearly ruled out by LHC run I constraints. This produced 10^5 representative samples to which the LHC SUSY searches have been applied. The ensuing $\sim 10^4$ samples that pass LHC run I constraints are displayed in figure 1.

4 Results

Our global fits identify two distinct viable solutions in the pMSSM parameter space (figure 1): the first exhibits a WIMP mass of $\sim 80 - 100$ GeV, with the neutralino annihilating to WW with a 95% branching ratio. The second solution has a larger neutralino mass, $\sim$

JCAP04(2016)037

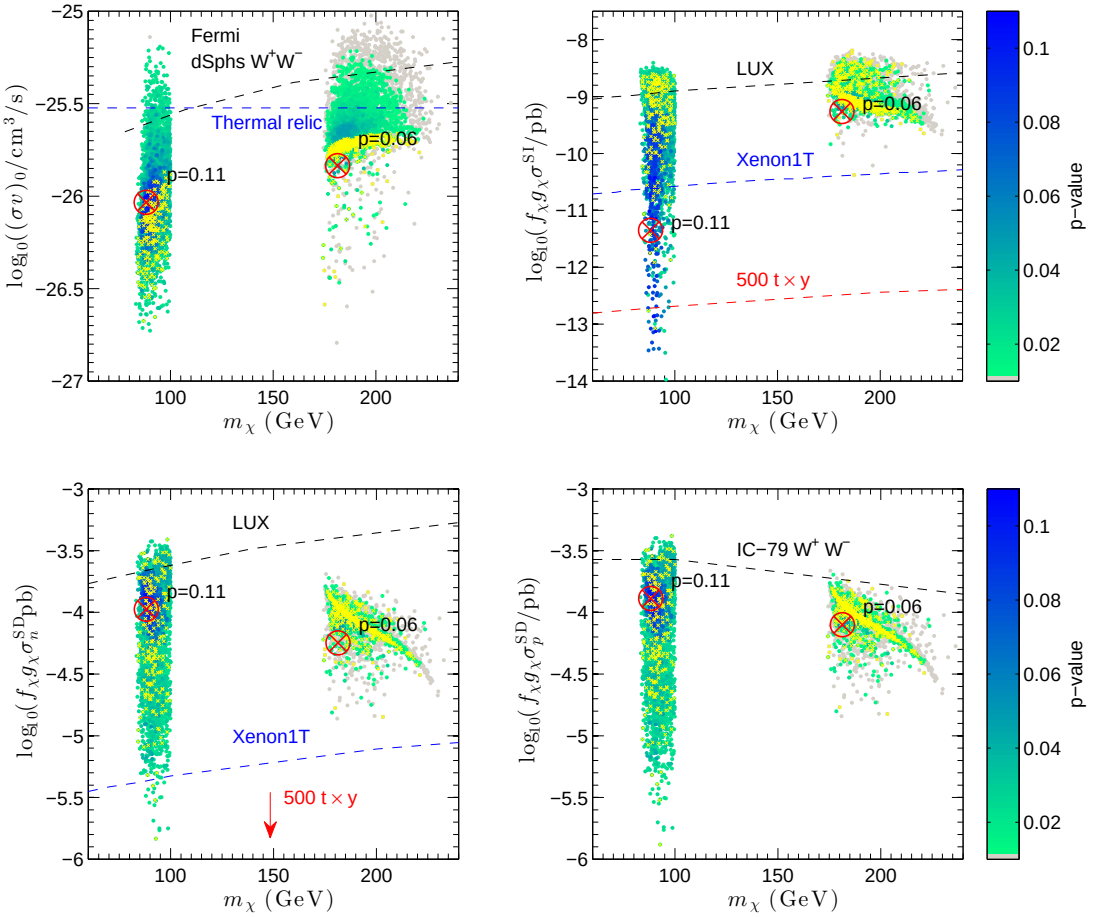

Figure 1. 2D map of the p-values of our fit, showing the annihilation (top left), the spin-independent (top right) and the spin-dependent (bottom panel, left for neutrons scattering and right for protons) cross-sections vs neutralino mass. The color-bar represents the p-value from the global fit. The yellow overlay highlights points that are within 2σ of the *Planck* relic density. Red crosses indicate the best-fit points in the two islands. The *Fermi* dwarfs limit for the W^+W^- channel [59] is plotted for reference only, and it has not been applied. To compare with *Fermi* dwarfs data, the annihilation cross-section needs to be rescaled by a factor f_χ^2, which would suppress the signal well below current limits. The spin-dependent and spin-independent cross-sections have been multiplied by $f_\chi = \Omega_\chi/\Omega_{\mathrm{DM}}$ and $g_\chi = \rho_0/0.3\,\mathrm{GeV/cm}^3$ to facilitate comparison with current and future limits (LUX [42], Xenon1T and a multi-ton liquid Xe detector with 500 t× yr exposure [61]). In the bottom right panel, we display the IC-79 limit [46] used in our analysis.

$180 - 200\,\mathrm{GeV}$, and 87% $\bar{t}t$ annihilation final states. The overall best-fit point is in the WW region has $-2\ln\mathcal{L} \equiv \chi^2 = 122.0$. This is for a fit with 21 free parameters, and 125 Gaussian data points (we do not include limits as their χ^2 is normalized to 0 whenever the constraint is satisfied), so we adopt 104 degrees of freedom.[1] Our best fit thus has a p-value of 0.11 versus a $\chi^2 = 127.6$ and a p-value of 0.06 for the $\bar{t}t$ solution.

[1]We emphasize that the calculation of the number of actual degrees of freedom is not trivial. One would have to consider the number of *active* data points, as well as the number of *effective* parameters in the model. This can only be done properly via extensive Monte Carlo simulations of the data. The simple counting argument we adopt is meant to be representative of what one would get in the simplest scenario.

JCAP04(2016)037

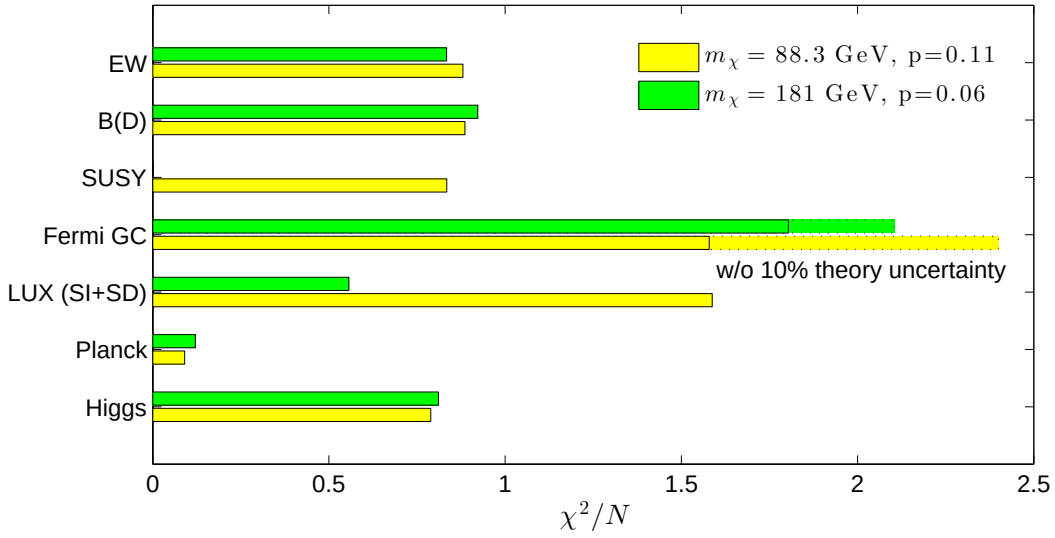

Figure 2. Contribution to the overall χ^2 for the two best-fit points, grouped by type of observable (see section 3 for details). The pulls have been normalized by the number of data points in each group, N, to facilitate a visual comparison. The dashed bars show the Galactic Centre *Fermi* likelihood contribution when the 10% theoretical uncertainty is neglected, which would degrade the p-values to 0.023 (for the $m_\chi = 88.3\,\text{GeV}$ solution) and 0.008 (for the $m_\chi = 188\,\text{GeV}$ model).

It is important to notice that including theoretical uncertainties in the GC fit is crucial in achieving reasonable p-values. The 10% theoretical uncertainty advocated in [32] is a reasonable reflection of the differences in the predicted spectra between current numerical codes. However, in absence of such an uncertainty, the quality of our global fit would degrade to 0.023 and 0.008 for the two best-fit points, respectively.

The contribution to the overall χ^2 for the two best-fit points from different types of observables are plotted in figure 2. The pulls have been normalized by the number of data points in each group, N, to facilitate a visual comparison. We notice that the χ^2 per data point is distributed fairly evenly across observables. There is a slight preponderance in the χ^2 contribution coming from the GC *Fermi* fit (with $N = 24$ bins), which is exacerbated if one neglects the 10% theoretical uncertainty in the DM spectra (dashed bars). The contribution to the pull from the LUX likelihood comes almost exclusively from the SD neutron cross-section limit, as the SI constraint is easily satisfied by our best-fit points.

Let us now analyze in more detail both type of solutions.

In the WW region, model points providing a better fit have a neutralino mostly bino-like ($\sim$ 80–90%) with a similar fraction of both wino and higgsino. Besides we find points in which neutralinos can be dominantly higgsinos with a bino fraction as small as $\sim$ 10%. Those provide a worse fit though, because a large higgsino composition, basically, implies a large annihilation cross section which drops the relic density below the Planck limit leading to a tension with the *Fermi* GeV excess due to the scaling Ansatz given in eq. (3.2).

Analogously to ref. [32], also in the present work, we find a WW solution with a bino-higgsino neutralino composition of about 84–92 GeV. However, in our work, this solution has a slightly worse χ^2 than in ref. [32]. The reason for this is that we adopt slightly different values of the form-factors for the computation of the SD cross-section. Since such a WW solution is now just below the WW IceCube limits, it is punished a bit in the likelihood.

JCAP04(2016)037

Typically, since third generation squarks enter into the SI cross section at loop level through LSP-gluon effective interactions [62], their contribution can be comparable to tree-level effective interactions mediated by squarks of the first two families when they are light. In this type of solutions, because current constraints allow sbottoms of a few hundred GeV, their contribution can be sizable and, indeed, cancels out the Higgs exchange contributions. This effect allows to relax the tension with LUX data when Higgs exchange contributions are large.

In terms of the impact of LHC run I data, we notice that first and second generation squarks as well as gluinos are decoupled. The stops and the heavier sbottom mass eigenstates are also kinematically inaccessible at the LHC Run-I energies. However, the lighter sbottom eigenstate with a mass around 400 GeV can be produced at the LHC at a considerable rate but the sbottoms evade detection from third generation searches due to complicated cascade decays. The sparticles in the electroweak sector are relatively light. There is a large mass splitting between the SU(2) doublet and singlet sleptons. The SU(2) doublet sleptons are light with masses around 250 GeV and narrowly evade detection in searches for two lepton and large missing transverse momentum final states. The lightest wino-like chargino and the second lightest neutralino escape detection since they are almost mass degenerate with the bino-like neutralino. The production rate of the higgsino eigenstates is too small to yield an observable signal at the LHC run I.

Results about the annihilation cross-section are shown in the top left panel of figure 1. One can see that the points with a better fit exhibit $\langle\sigma v\rangle \sim 10^{-26}$ cm^3/s, consistent with the results found in [15]. We also show the *Fermi* dwarfs limit for the W^+W^- channel [59], but we emphasize that this limit has not been applied in the fit. In order to compare with the constraint coming from *Fermi* dwarfs observations, the annihilation cross-section needs to be rescaled by a factor f_χ^2 (to account for the possibility of sub-dominant dark matter relic density, which translates according to our Ansatz in a correspondingly reduced local density in the dwarfs), which would suppress the signal well below current and future limits from dwarfs.

Regarding DM direct detection, the top right panel of figure 1 shows the SI cross-section versus neutralino mass plane. In order to facilitate the visual comparison of our pMSSM models with existing and future limits, we have rescaled the theoretical cross-section by a factor f_χ (to account for models where the neutralino does not make up all of the cosmological relic density) and a factor $g_\chi \equiv \rho_0/0.3\,\mathrm{GeV/cm^3}$. This accounts for the fact that the local density we have used to predict the number of counts for LUX, ρ_0, is a nuisance parameter which is generally different from the value assumed by the LUX collaboration in deriving their limit [42], namely $0.3\,\mathrm{GeV/cm^3}$.

The points that appear above the nominal 95% exclusion limit from LUX cannot be excluded because of a combination of effects: (i) our LUX likelihood is slightly less stringent than what has been published by the LUX collaboration (and depicted in figure 1), (ii) our likelihood function for LUX allows for values of the cross section above the 95% limit to be included (albeit penalized by a smaller likelihood value), and (iii) the global likelihood function can — to an extent — compensate for a poor fit to LUX data by gaining an improvement from other data sets.

Since squarks are heavy, the contribution coming from the exchange of a CP-even Higgs dominates and therefore the SI cross-section scales as $\propto |N_{11}N_{13/14}|^2$. Because, as noticed above, the higgsino fraction in this region is not negligible, it can be large. Indeed, there are model points above the LUX limit allowed by the scaling Ansatz we apply to the local dark matter density and to some extend due to the fact that we vary the local dark matter density. Another interesting feature is that the SI cross-section spans down to $\sim 10^{-14}$ pb. That is

JCAP04(2016)037

possible because the heavy CP-even Higgs contribution can be sizable and cancellations with the lightest Higgs channel might occur [63].

In the bottom panels of figure 1 we display the SD cross-section for scattering off neutrons/protons (left/right panels). While in the case of SI interactions the contributions for proton and neutron are comparable, the SD cross-sections may differ significantly. However, we find a tight correlation between the SD cross-sections for scattering off neutrons and those off protons in our model points. The SD cross-section is dominated by the exchange of a Z boson and therefore the SD cross-section is largely determined by the higgsino content of the neutralino and likewise for the SI cross-section it can be sizable in this region as it can be seen in both panels.

In terms of dark matter direct detection experiments, at present, LUX data represents the strongest constraint on the SD-neutron scattering cross-section because the Xenon contains neutron-odd isotopes therefore we overlay the LUX constraint properly rescaled as for the SI case. For the SD-proton scattering cross-section, IC-79 represents the strongest current constraint for the particular case when the neutralinos annihilate to a W^+W^- final state so we show the IC-79 90% CL upper limit [46] , and we have rescaled the value of the SD cross-section by a factor f_χ. This assumes that equilibrium between capture and annihilation is reached in the Sun, which is a good assumption for the bulk of the models shown here. In fact, in the region where the neutralino annihilates mainly to WW and to ZZ to a lesser extend, the IC-79 limits apply here and disfavor a large number of model points.

One can see that there are model points above LUX and IC-79 exclusion lines. In those, the higgsino component of the neutralino is dominant over the gaugino one leading to a large SD cross-section for both neutrons and protons. Those points still provide a reasonable fit to the data due to two effects, first because neutralinos with a large higgsino component yield to a relic density sensibly below the Planck bound and therefore the scaling Ansatz applies and second because the local dark matter density is a nuisance parameter in our analysis. Beside there is a small fraction of points above the nominal IC-79 WW limit with a branching ratio to WW and ZZ low enough to evade the stringent IC-79 bound.

In the $\bar{t}t$ region, points providing a better fit have a neutralino dominantly bino-like ($\sim 90\%$) with a $\sim 10\%$ of higgsino. Those points have the characteristic that the neutralinos annihilate to top quark pairs via an exchange of a right-handed stop which is relatively heavy ($\sim 1\,\text{TeV}$). This is possible because on top of the non-helicity suppression the neutralino-stop-top coupling component, which is proportional to the top quark Yukawa coupling, is sizeable due to the non-vanishing higgssino fraction of the neutralino. We also found points in which the right-handed stops are light ($\sim 300\,\text{GeV}$) being almost bino-like (also found in [32]). However those provide a worse fit to the $BR(\bar{B} \to X_s\gamma)$ data because higgssino-stop loops have a sizable positive contribution which leads to values above the experimental constraint.

Annihilation into $t\bar{t}$ through a t-channel stop exchange requires, for bino-like neutralinos, stops with masses of a few hundred GeV. On the other hand, relatively light stops are not able to lift the tree-level Higgs mass to fit a 125 GeV Higgs. In order to enhance the DM annihilation cross sections to match the Planck measurement, the neutralino coannihilates with sneutrinos which have to be about the same mass as the DM particle ($\sim 200\,\text{GeV}$). This induces the splitting in the left/right sleptons spectrum.

These benchmark points are characterized by left handed slepton next-to-lightest supersymmetric particle with masses above 200 GeV. The higgsinos have masses around 260 GeV. Since the resulting mass differences between the bino-like LSP and the sleptons/higgsinos are small, the final states are rather soft and thus the detection is suppressed in events with

JCAP04(2016)037

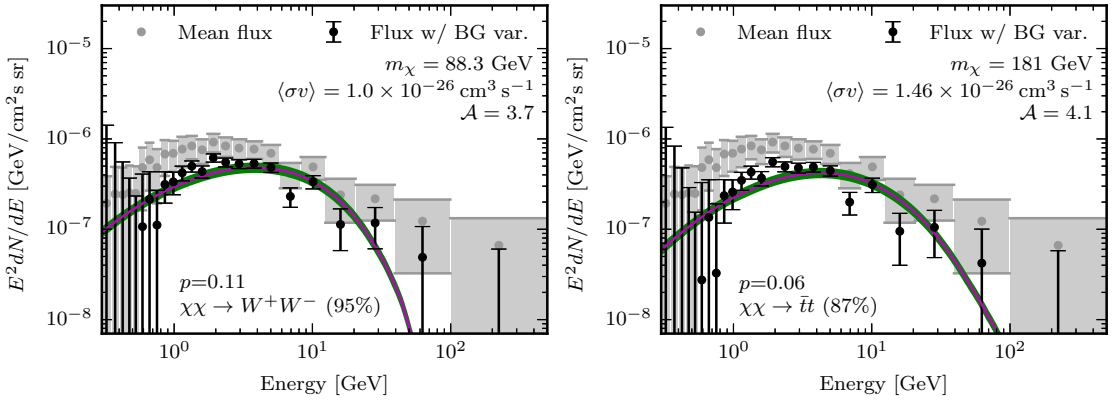

Figure 3. Spectral energy distribution of the *Fermi*-GeV excess data. *Grey dots* show *Fermi* GeV excess mean values w.r.to background model variations, together with associated systematic uncertainties (*grey boxes*). *Black dots* represent the excess for a variation of the Galactic diffuse emission contribution (within its systematic uncertainty). The solid lines show the prediction for the pMSSM models that give the best fits in the two regions of figure 1 and have dominant annihilation channel into W bosons or top quarks (*magenta lines* in the left and right panel, respectively). The *green lines* indicate the adopted 10% systematic uncertainties in the spectra. Furthermore, $\mathcal{A}$ denotes the required boost-factor with respect to a generalized Navarro-Frenk-White DM density profile with inner slope γ=1.26. The p denotes the p-value of the global fit (including all data).

dilepton or trilepton final states and large missing transverse energy momentum. The production rate of the sbottom is quite suppressed and hence avoids detection. The spectrum of the remaining supersymmetric particles is decoupled.

The phenomenology of the model points in the $\bar{t}t$ region in terms of DM detection is similar to the WW one. The main difference is in that the IC-79 limits does not apply and therefore larger SD cross-sections are possible. The main difference is that the higgsino composition is not as large as in the WW type of solutions and therefore the SD cross sections for neutron interactions are below the LUX current sensitivity.

Lastly, in figure 3, we show the spectrum of the *Fermi* GeV excess together with the systematic uncertainties associated with the galactic diffuse emission modeling [15]. We compare the data with the spectra of the pMSSM model points giving the best global p-value in the two regions identified in figure 1.

It is apparent from figure 3 that the best-fit DM spectra are systematically offset from the mean values of the Galactic center excess spectrum (gray dots and boxes), by about 1 to 2 sigma, and do not provide a good fit to the data at first sight. However, since the systematic astrophysical uncertainties, indicated by the gray boxes ($\pm 1\sigma$) are *correlated*, this still provides an acceptable fit to the data. To *illustrate* this point, we show with black dots and error bars the excess spectrum where we moved all data points systematically down, according to the freedom allowed by the covariance (the error bars show now statistical errors only). Together with the 10% uncorrelated systematic modeling uncertainty that we adopted for the DM signal, this provides a reasonable fit to the data, with p-values, whereas without the DM signal modeling uncertainties, the p-values would be prohibitively small (see figure 2 above).

JCAP04(2016)037

5 Discovery potential: dark matter detection experiments and LHC run II

5.1 Implications for direct and indirect dark matter searches

Generally, SD and SI scattering cross sections are driven by the higgsino content of the neutralino. Therefore, as explained above, the sizable higgsino fraction of points in the two best-fit regions imply large SI cross-sections that makes the direct detection prospects promising, although the SI cross-section range spans down to $\sim 10^{-14}$ pb due to cancellations with the lightest Higgs. In figure 1, top right panel, we also display the projected sensitivity limit (defined as the 90% CL exclusion limit) for the Xenon1T experiment and an hypothetical liquid Xe detector with 500 t$\times$ yr exposure [61]. The latter experiment essentially saturates the ultimate detection floor set by coherent neutrino scattering [64]. Xenon1T data will be crucial in discovering or firmly ruling out models belonging to the $\bar{t}t$ island and will probe a significant fraction of the parameter space preferred by the first type of solutions. In figure 1, bottom left panel, we overlay the projected 90% exclusion limit for Xenon1T [61]. We find that Xenon1T will be able to prove the entirety of the SD neutron scattering cross-section parameter space favoured by our models.[2] A multi-ton experiment with 500 t$\times$ yr exposure would reach sensitivities a couple of order of magnitudes smaller than the smallest SD neutron cross-sections found in our scan.

The bottom right panel of figure 1 shows that our best-fit points easily evade the constraint set by IC-79 on the SD proton cross-section in the implementation we adopted in this paper. However, an event-level implementation of the likelihood (including the events' energies [66]) would increase the constraining power of the IC-79 limit, to the point that some of the surviving models could be probed [67].

Finally, as for indirect detection, the preferred parameter space is mostly out of reach even for the future 10-yr *Fermi* analysis of dwarf spheroidal galaxies [68], where a further improvement of current sensitivities by a factor 2–3 can be expected. Note that points with a large annihilation cross section as shown in the top right panel of figure 1 usually correspond to suppressed relic densities, making these points hard to detect due to the f_χ^2 factor suppression of their signal.

5.2 Prospects for detection at the LHC run II

The models yielding the best p-values show several interesting properties relevant for LHC searches. In the following we briefly discuss the discovery prospects depending on the produced SUSY particles. Sparticle mass distributions and MSSM parameters relevant for LHC searches are shown in figure 4.

Light squarks: in the top left panel of figure 4 we plot the lightest first/second generation squark mass vs the neutralino mass. The first and second generation squarks have masses $>$ 1400 GeV, i.e. above the usual run I constraints. About 70% of the models have squark masses below 2000 GeV.[3] The upcoming run II searches for light squarks will exclude many scenarios. In almost all models the left- and right-handed squarks have different branching ratios and

[2] We note that the Xenon1T exclusion limits in [61] are obtained by applying a scaling factor derived from the comparison between SI and SD results of Xenon100 and result to be slightly stronger than the limits quoted in ref. [65], which instead adopts a 60 times improvement w.r.to XENON100 (still Xenon1T will be able to entirely probe our identified parameter space).

[3] The expected reach of the ATLAS and CMS experiments for full MSSM models is not estimated. We compare with mass scales which are likely excluded with HL-LHC data for many MSSM scenarios.

JCAP04(2016)037

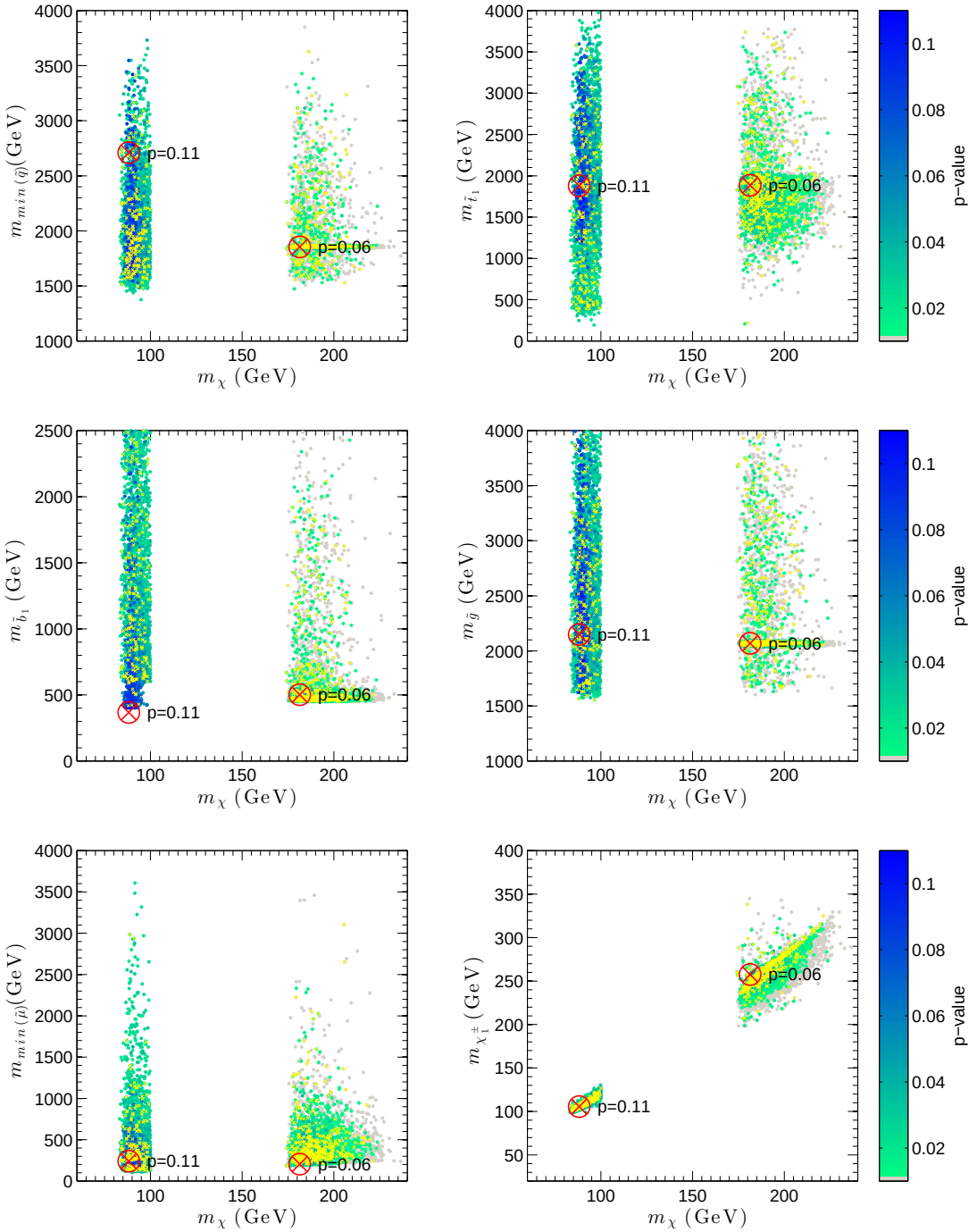

Figure 4. 2D map of the p-values of our fit, showing the lightest squark mass of the first and second generation (top left), the lightest stop (top right), the lightest sbottom (middle left), the gluino (middle right), the lightest smuon (bottom left) and the lightest chargino (bottom right) vs the neutralino mass. The yellow overlay shows points within 2σ of the *Planck* relic density value.

JCAP04(2016)037

tend to decay to the heavy neutralino and chargino states. Cascade decays including W, Z and Higgs bosons are common.

Stop: in the top right panel of figure 4 we plot the stop mass vs the neutralino mass. Some models have light stops with masses down to 200–300 GeV decaying to chargino and a b-jet. The neutralino has a mass of around 95 GeV. These models are not excluded by current LHC searches [69]. Another interesting region also found in [32] has a stop mass of around 200–220 GeV and a mass of the lightest neutralino around 180 GeV. A slight excess in the ATLAS data prevents exclusion with run I data in this region [69]. These solutions will likely be tested with early run II analyses. Other solutions yield much heavier stop masses decaying predominantly into the heavier neutralino and chargino states. Dedicated searches for such decays are important.

Sbottom: in the central left panel of figure 4 we plot the sbottom mass vs the neutralino mass. Several model points have a sbottom mass as low as 400 GeV. The points are not excluded in our procedure due to multi-step cascade decays involving heavy neutralinos.

Typically, the lighter sbottom state has masses around 400 GeV while the lightest neutralino is mostly bino-like with a mass around 90 GeV. The second lightest wino-like neutralino lies around 107 GeV. The two heavier neutralinos are higgsino dominated states and have masses around 250 GeV.

If the sbottoms predominantly decayed into a bottom quark and the lightest neutralino, these benchmark points would clearly be excluded. However, the bottom squark decays into all four neutralino as well as the lighter chargino mass eigenstates with comparable rates. The decay modes of the neutralino and chargino mass eigenstates are relatively complex and hence the limits from simplified sbottom searches do not apply. For instance, the second lightest neutralino eigenstate has large hadronic three body decay modes into the lightest neutralino via off shell Z bosons. Moreover, the second lightest neutralino can radiatively decay into a photon and the lightest neutralino. The corresponding lighter chargino eigentstate has relatively large leptonic three body decay modes via off shell W bosons. Finally, the two heaviest higgsino dominated neutralino mass eigenstates mainly decay into electroweak gauge bosons and the lighter electroweakino states. As a consequence, many events have leptons in the final state which are vetoed in the searches for direct sbottom production. In addition, the higher final state multiplicity tends to soften the net missing transverse momentum distribution compared to scenarios with direct sbottom decays into a bottom quark and the LSP. As a result fewer events pass the selection cuts of the relevant sbottom searches. We explicitly tested those light sbottom scenarios against experimental searches at the LHC with the computer tool CheckMATE and confirmed that those points were allowed.

As seen also for the light squarks about 70% of the models would be excluded with a sbottom limit of ≈ 1000 GeV.

Gluinos: in the central right panel of figure 4 we plot the sbottom mass vs the neutralino mass. Gluinos have masses > 1600 GeV. An upcoming early run II exclusion on gluinos with a mass up to 2500 GeV would exclude about 15% of these models. Run II searches for first and second generation squarks will thus likely be more constraining.

Sleptons: in the bottom left panel of figure 4 we plot the lightest smuon mass vs the neutralino mass. The lightest smuons found in the best fit models have masses < 400 GeV in about 60% of the best fit points. This makes searches for smuons in run II very sensitive to these solutions.

JCAP04(2016)037

Chargino/neutralino: in the bottom right panel of figure 4 we plot the chargino mass vs the neutralino mass. Due to the GeV excess likelihood several neutralinos and charginos are typically light, the lightest having a mass fixed to $80 - 100\,\mathrm{GeV}$ for the WW solutions and $180 - 200\,\mathrm{GeV}$ for the $\bar{t}t$ solutions. The higgsino component in the $\bar{t}t$ and WW solutions typically involves that μ is only slightly larger than these mass scales, leading to 2 more neutralinos and the light chargino at masses around $100\,\mathrm{GeV}$ (WW) or 200–$300\,\mathrm{GeV}$ ($\bar{t}t$). These states are often mass compressed with the lightest neutralino which makes the solutions evade LHC chargino/neutralino searches so far. Dedicated chargino/neutralino searches will have sensitivity to most models, e.g. by a mono-jet and soft lepton search as proposed also in ref. [32]. The Wino mass scale is quite unconstrained and lies between $100\,\mathrm{GeV}$ and $1.5\,\mathrm{TeV}$. The Wino will decay to lighter states yielding final states with Z, W or Higgs bosons.

Heavy Higgs: about 50% of the best models have $m_A < 800\,\mathrm{GeV}$ making searches for heavy Higgs bosons very sensitive. Several chargino and neutralino states are light and have a large coupling to $A/H/H^{\pm}$. Consequently heavy Higgs decays to charginos and neutralinos can have huge branching ratios up to 30% competing with top and bottom decays. Dedicated searches for heavy Higgs bosons decaying into final states with $W/Z/h$ with missing transverse momentum would help to constrain these scenarios.

6 Conclusions

In this paper we addressed the issue of finding model points in the pMSSM that might explain simultaneously the large set of independent data we gathered from astrophysics, cosmology and high-energy particle physics. We showed that no tension exists between currently available particle physics constraints and the interpretation of the *Fermi* GeV excess in terms of dark matter annihilation in the framework of the pMSSM. Furthermore, we found evidence for two regions that are able to explain the gamma-ray data, while being consistent with other various experimental constraints: (a) a first region where the neutralino is mostly bino-like and the dominant annihilation channel today is 95% into W bosons pairs and (b) a second region where the the annihilation into top-quark pairs dominates and the neutralino is again mainly bino-like. We showed that these models are very appealing since they will be soon in the reach of the next generation of direct detection experiments — Xenon1T will probe the entirety of the best-fit regions thanks to its sensitivity to spin-dependent neutron cross-section — and of the LHC run II, in particular through searches for charginos and neutralinos, squarks and light smuons.

Acknowledgments

We warmly thank T. Bringmann, Marco Selvi, Christopher McCabe, Pat Scott and Tim Stefaniak for useful discussions, Marc Schumann and Marco Selvi for providing us with direct detection limits and William Parker for assistance with some figures. G.B. (P.I.) and F.C. acknowledge support from the European Research Council through the ERC starting grant WIMPs Kairos. R. RdA, is supported by the Ramón y Cajal program of the Spanish MICINN and also thanks the support of the Spanish MICINN's Consolider-Ingenio 2010 Programme under the grant MULTIDARK CSD2209-00064, the Invisibles European ITN project (FP7-PEOPLE-2011-ITN, PITN-GA-2011-289442-INVISIBLES and the "SOM Sabor y origen de la Materia" (FPA2011-29678) and the "Fenomenologia y Cosmologia de la Fisica mas

JCAP04(2016)037

alla del Modelo Estandar e lmplicaciones Experimentales en la era del LHC" (FPA2010-17747) MEC projects. The work of J. S. Kim has been partially supported by the MINECO, Spain, under contract FPA2013-44773-P; Consolider-Ingenio CPAN CSD2007-00042 and the Spanish MINECO Centro de excelencia Severo Ochoa Program under grant SEV-2012-0249. R.T. acknowledges partial support from an EPSRC "Pathways to Impact" grant. C.W. was supported by the Netherlands Organization for Scientific Research (NWO) through a Vidi grant. We gratefully acknowledge the use of the Cartesius supercomputer (Amsterdam) and of Imperial College London's HPC. This work was supported by Grant ST/N000838/1 from the Science and Technology Facilities Council.

References

[1] G. Jungman, M. Kamionkowski and K. Griest, *Supersymmetric dark matter*, *Phys. Rept.* **267** (1996) 195 [hep-ph/9506380] [INSPIRE].

[2] L. Bergström, *Nonbaryonic dark matter: observational evidence and detection methods*, *Rept. Prog. Phys.* **63** (2000) 793 [hep-ph/0002126] [INSPIRE].

[3] G. Bertone, D. Hooper and J. Silk, *Particle dark matter: evidence, candidates and constraints*, *Phys. Rept.* **405** (2005) 279 [hep-ph/0404175] [INSPIRE].

[4] G. Bertone ed., *Particle dark matter: observations, models and searches*, Cambridge University Press, Cambridge U.K. (2010).

[5] PLANCK collaboration, J. Tauber et al., *The scientific programme of Planck*, astro-ph/0604069 [INSPIRE].

[6] L. Goodenough and D. Hooper, *Possible evidence for dark matter annihilation in the inner milky way from the Fermi gamma ray space telescope*, arXiv:0910.2998 [INSPIRE].

[7] FERMI-LAT collaboration, V. Vitale and A. Morselli, *Indirect search for dark matter from the center of the milky way with the Fermi-Large Area Telescope*, arXiv:0912.3828 [INSPIRE].

[8] D. Hooper and L. Goodenough, *Dark matter annihilation in the galactic center as seen by the Fermi gamma ray space telescope*, *Phys. Lett.* **B 697** (2011) 412 [arXiv:1010.2752] [INSPIRE].

[9] D. Hooper and T. Linden, *On the origin of the gamma rays from the galactic center*, *Phys. Rev.* **D 84** (2011) 123005 [arXiv:1110.0006] [INSPIRE].

[10] K.N. Abazajian and M. Kaplinghat, *Detection of a gamma-ray source in the galactic center consistent with extended emission from dark matter annihilation and concentrated astrophysical emission*, *Phys. Rev.* **D 86** (2012) 083511 [*Erratum ibid.* **D 87** (2013) 129902] [arXiv:1207.6047] [INSPIRE].

[11] C. Gordon and O. Macias, *Dark matter and pulsar model constraints from galactic center Fermi-LAT gamma ray observations*, *Phys. Rev.* **D 88** (2013) 083521 [*Erratum ibid.* **D 89** (2014) 049901] [arXiv:1306.5725] [INSPIRE].

[12] D. Hooper and T.R. Slatyer, *Two emission mechanisms in the Fermi bubbles: a possible signal of annihilating dark matter*, *Phys. Dark Univ.* **2** (2013) 118 [arXiv:1302.6589] [INSPIRE].

[13] K.N. Abazajian, N. Canac, S. Horiuchi and M. Kaplinghat, *Astrophysical and dark matter interpretations of extended gamma-ray emission from the galactic center*, *Phys. Rev.* **D 90** (2014) 023526 [arXiv:1402.4090] [INSPIRE].

[14] T. Daylan et al., *The characterization of the gamma-ray signal from the central milky way: a case for annihilating dark matter*, *Phys. Dark Univ.* **12** (2016) 1 [arXiv:1402.6703] [INSPIRE].

[15] F. Calore, I. Cholis and C. Weniger, *Background model systematics for the Fermi GeV excess*, *JCAP* **03** (2015) 038 [arXiv:1409.0042] [INSPIRE].

JCAP04(2016)037

[16] Fermi-LAT collaboration, S. Murgia, *Observations of high-energy gamma-ray emission toward the galactic center*, talk given at the 2014 *Fermi Symposium*, Nagoya Japan October 20–24 2014.

[17] F. Calore, I. Cholis, C. McCabe and C. Weniger, *A tale of tails: dark matter interpretations of the Fermi GeV excess in light of background model systematics*, *Phys. Rev.* **D 91** (2015) 063003 [arXiv:1411.4647] [INSPIRE].

[18] K.N. Abazajian, *The consistency of Fermi-LAT observations of the galactic center with a millisecond pulsar population in the central stellar cluster*, *JCAP* **03** (2011) 010 [arXiv:1011.4275] [INSPIRE].

[19] F. Calore, M. Di Mauro, F. Donato and F. Donato, *Diffuse gamma-ray emission from galactic pulsars*, *Astrophys. J.* **796** (2014) 1 [arXiv:1406.2706] [INSPIRE].

[20] Q. Yuan and B. Zhang, *Millisecond pulsar interpretation of the galactic center gamma-ray excess*, *JHEAp* **3-4** (2014) 1 [arXiv:1404.2318] [INSPIRE].

[21] J. Petrović, P.D. Serpico and G. Zaharijas, *Millisecond pulsars and the galactic center gamma-ray excess: the importance of luminosity function and secondary emission*, *JCAP* **02** (2015) 023 [arXiv:1411.2980] [INSPIRE].

[22] E. Carlson and S. Profumo, *Cosmic ray protons in the inner galaxy and the galactic center gamma-ray excess*, *Phys. Rev.* **D 90** (2014) 023015 [arXiv:1405.7685] [INSPIRE].

[23] J. Petrović, P.D. Serpico and G. Zaharijaš, *Galactic center gamma-ray "excess" from an active past of the galactic centre?*, *JCAP* **10** (2014) 052 [arXiv:1405.7928] [INSPIRE].

[24] I. Cholis, C. Evoli, F. Calore, T. Linden, C. Weniger and D. Hooper, *The galactic center GeV excess from a series of leptonic cosmic-ray outbursts*, *JCAP* **12** (2015) 005 [arXiv:1506.05119] [INSPIRE].

[25] D. Gaggero, M. Taoso, A. Urbano, M. Valli and P. Ullio, *Towards a realistic astrophysical interpretation of the gamma-ray galactic center excess*, *JCAP* **12** (2015) 056 [arXiv:1507.06129] [INSPIRE].

[26] R. Bartels, S. Krishnamurthy and C. Weniger, *Strong support for the millisecond pulsar origin of the galactic center GeV excess*, *Phys. Rev. Lett.* **116** (2016) 051102 [arXiv:1506.05104] [INSPIRE].

[27] S.K. Lee, M. Lisanti, B.R. Safdi, T.R. Slatyer and W. Xue, *Evidence for unresolved γ-ray point sources in the inner galaxy*, *Phys. Rev. Lett.* **116** (2016) 051103 [arXiv:1506.05124] [INSPIRE].

[28] T.D. Brandt and B. Kocsis, *Disrupted globular clusters can explain the galactic center gamma ray excess*, *Astrophys. J.* **812** (2015) 15 [arXiv:1507.05616] [INSPIRE].

[29] MSSM Working Group collaboration, A. Djouadi et al., *The minimal supersymmetric standard model: group summary report*, hep-ph/9901246 [INSPIRE].

[30] M. Cahill-Rowley, J. Gainer, J. Hewett and T. Rizzo, *Towards a supersymmetric description of the Fermi galactic center excess*, *JHEP* **02** (2015) 057 [arXiv:1409.1573] [INSPIRE].

[31] P. Agrawal, B. Batell, P.J. Fox and R. Harnik, *WIMPs at the galactic center*, *JCAP* **05** (2015) 011 [arXiv:1411.2592] [INSPIRE].

[32] A. Achterberg, S. Amoroso, S. Caron, L. Hendriks, R. Ruiz de Austri and C. Weniger, *A description of the galactic center excess in the minimal supersymmetric standard model*, *JCAP* **08** (2015) 006 [arXiv:1502.05703] [INSPIRE].

[33] ATLAS, CDF, CMS and D0 collaborations, *First combination of Tevatron and LHC measurements of the top-quark mass*, arXiv:1403.4427 [INSPIRE].

JCAP04(2016)037

[34] M. Pato, L. Baudis, G. Bertone, R. Ruiz de Austri, L.E. Strigari and R. Trotta, *Complementarity of dark matter direct detection targets*, *Phys. Rev.* **D 83** (2011) 083505 [arXiv:1012.3458] [INSPIRE].

[35] G. Bertone, D.G. Cerdeno, M. Fornasa, R.R. de Austri and R. Trotta, *Identification of dark matter particles with LHC and direct detection data*, *Phys. Rev.* **D 82** (2010) 055008 [arXiv:1005.4280] [INSPIRE].

[36] SLD Electroweak Group, DELPHI, ALEPH, SLD, SLD Heavy Flavour Group, OPAL, LEP Electroweak Working Group and L3 collaborations, S. Schael et al., *Precision electroweak measurements on the Z resonance*, *Phys. Rept.* **427** (2006) 257 [hep-ex/0509008] [INSPIRE].

[37] C. Strege et al., *Profile likelihood maps of a* 15*-dimensional MSSM*, *JHEP* **09** (2014) 081 [arXiv:1405.0622] [INSPIRE].

[38] A. Arbey, M. Battaglia, F. Mahmoudi and D. Martínez Santos, *Supersymmetry confronts* $B_s \to \mu^+\mu^-$*: present and future status*, *Phys. Rev.* **D 87** (2013) 035026 [arXiv:1212.4887] [INSPIRE].

[39] CMS and LHCb collaborations, *Combination of results on the rare decays* $B^0_{(s)} \to \mu^+\mu^-$ *from the CMS and LHCb experiments*, CMS-PAS-BPH-13-007, CERN, Geneva Switzerland (2013) [LHCb-CONF-2013-012] [CERN-LHCb-CONF-2013-012].

[40] G. Bertone, K. Kong, R.R. de Austri and R. Trotta, *Global fits of the minimal universal extra dimensions scenario*, *Phys. Rev.* **D 83** (2011) 036008 [arXiv:1010.2023] [INSPIRE].

[41] Planck collaboration, P.A.R. Ade et al., *Planck* 2013 *results. XVI. Cosmological parameters*, *Astron. Astrophys.* **571** (2014) A16 [arXiv:1303.5076] [INSPIRE].

[42] LUX collaboration, D.S. Akerib et al., *First results from the LUX dark matter experiment at the Sanford Underground Research Facility*, *Phys. Rev. Lett.* **112** (2014) 091303 [arXiv:1310.8214] [INSPIRE].

[43] C. Savage, A. Scaffidi, M. White and A.G. Williams, *LUX likelihood and limits on spin-independent and spin-dependent WIMP couplings with LUXCalc*, *Phys. Rev.* **D 92** (2015) 103519 [arXiv:1502.02667] [INSPIRE].

[44] QCDSF collaboration, G.S. Bali et al., *Strangeness contribution to the proton spin from lattice QCD*, *Phys. Rev. Lett.* **108** (2012) 222001 [arXiv:1112.3354] [INSPIRE].

[45] P. Junnarkar and A. Walker-Loud, *Scalar strange content of the nucleon from lattice QCD*, *Phys. Rev.* **D 87** (2013) 114510 [arXiv:1301.1114] [INSPIRE].

[46] IceCube collaboration, M.G. Aartsen et al., *Search for dark matter annihilations in the sun with the* 79*-string IceCube detector*, *Phys. Rev. Lett.* **110** (2013) 131302 [arXiv:1212.4097] [INSPIRE].

[47] Super-Kamiokande collaboration, K. Choi et al., *Search for neutrinos from annihilation of captured low-mass dark matter particles in the sun by Super-Kamiokande*, *Phys. Rev. Lett.* **114** (2015) 141301 [arXiv:1503.04858] [INSPIRE].

[48] ANTARES collaboration, S. Adrian-Martinez et al., *First results on dark matter annihilation in the sun using the ANTARES neutrino telescope*, *JCAP* **11** (2013) 032 [arXiv:1302.6516] [INSPIRE].

[49] R.R. de Austri, R. Trotta and L. Roszkowski, *A Markov chain Monte Carlo analysis of the CMSSM*, *JHEP* **05** (2006) 002 [hep-ph/0602028] [INSPIRE].

[50] P. Bechtle et al., *HiggsBounds-*4*: improved tests of extended Higgs sectors against exclusion bounds from LEP, the Tevatron and the LHC*, *Eur. Phys. J.* **C 74** (2014) 2693 [arXiv:1311.0055] [INSPIRE].

JCAP04(2016)037

[51] ATLAS collaboration, *Observation of a new particle in the search for the standard model Higgs boson with the ATLAS detector at the LHC*, *Phys. Lett.* **B 716** (2012) 1 [arXiv:1207.7214] [INSPIRE].

[52] CMS collaboration, *Observation of a new boson at a mass of* 125 *GeV with the CMS experiment at the LHC*, *Phys. Lett.* **B 716** (2012) 30 [arXiv:1207.7235] [INSPIRE].

[53] P. Bechtle, S. Heinemeyer, O. Stål, T. Stefaniak and G. Weiglein, *HiggsSignals: confronting arbitrary Higgs sectors with measurements at the Tevatron and the LHC*, *Eur. Phys. J.* **C 74** (2014) 2711 [arXiv:1305.1933] [INSPIRE].

[54] A. Djouadi, M.M. Muhlleitner and M. Spira, *Decays of supersymmetric particles: the program SUSY-HIT (SUspect-SdecaY-HDECAY-InTerface)*, *Acta Phys. Polon.* **B 38** (2007) 635 [hep-ph/0609292] [INSPIRE].

[55] T. Sjöstrand et al., *An introduction to PYTHIA* 8.2, *Comput. Phys. Commun.* **191** (2015) 159 [arXiv:1410.3012] [INSPIRE].

[56] R.D. Ball et al., *Parton distributions with LHC data*, *Nucl. Phys.* **B 867** (2013) 244 [arXiv:1207.1303] [INSPIRE].

[57] M. Drees, H. Dreiner, D. Schmeier, J. Tattersall and J.S. Kim, *CheckMATE: confronting your favourite new physics model with LHC data*, *Comput. Phys. Commun.* **187** (2014) 227 [arXiv:1312.2591] [INSPIRE].

[58] DELPHES 3 collaboration, J. de Favereau et al., *DELPHES* 3*, a modular framework for fast simulation of a generic collider experiment*, *JHEP* **02** (2014) 057 [arXiv:1307.6346] [INSPIRE].

[59] FERMI-LAT collaboration, M. Ackermann et al., *Searching for dark matter annihilation from milky way dwarf spheroidal galaxies with six years of Fermi Large Area Telescope data*, *Phys. Rev. Lett.* **115** (2015) 231301 [arXiv:1503.02641] [INSPIRE].

[60] F. Feroz, M.P. Hobson and M. Bridges, *MultiNest: an efficient and robust Bayesian inference tool for cosmology and particle physics*, *Mon. Not. Roy. Astron. Soc.* **398** (2009) 1601 [arXiv:0809.3437] [INSPIRE].

[61] M. Schumann, L. Baudis, L. Bütikofer, A. Kish and M. Selvi, *Dark matter sensitivity of multi-ton liquid xenon detectors*, *JCAP* **10** (2015) 016 [arXiv:1506.08309] [INSPIRE].

[62] M. Drees and M. Nojiri, *Neutralino-nucleon scattering revisited*, *Phys. Rev.* **D 48** (1993) 3483 [hep-ph/9307208] [INSPIRE].

[63] V. Mandic, A. Pierce, P. Gondolo and H. Murayama, *The lower bound on the neutralino nucleon cross-section*, hep-ph/0008022 [INSPIRE].

[64] J. Billard, L. Strigari and E. Figueroa-Feliciano, *Solar neutrino physics with low-threshold dark matter detectors*, *Phys. Rev.* **D 91** (2015) 095023 [arXiv:1409.0050] [INSPIRE].

[65] M. Garny, A. Ibarra, M. Pato and S. Vogl, *On the spin-dependent sensitivity of XENON*100, *Phys. Rev.* **D 87** (2013) 056002 [arXiv:1211.4573] [INSPIRE].

[66] ICECUBE collaboration, P. Scott et al., *Use of event-level neutrino telescope data in global fits for theories of new physics*, *JCAP* **11** (2012) 057 [arXiv:1207.0810] [INSPIRE].

[67] ICECUBE collaboration, to appear (2015).

[68] T. Bringmann and C. Weniger, *Gamma ray signals from dark matter: concepts, status and prospects*, *Phys. Dark Univ.* **1** (2012) 194 [arXiv:1208.5481] [INSPIRE].

[69] ATLAS collaboration, *Search for top squark pair production in final states with one isolated lepton, jets and missing transverse momentum in* $\sqrt{s}$ *=8 TeV pp collisions with the ATLAS detector*, *JHEP* **11** (2014) 118 [arXiv:1407.0583] [INSPIRE].

JCAP04(2016)037